

4. Oyanagi A, Orikasa M, Kawachi H, *et al.* Crescent-forming mechanism in an irreversible Thy-1 model in rats. *Nephron* 2001; **89**: 439–447.
5. Cunningham MA, Ono T, Hewitson TD, Tipping PG, Becker GJ, Holdsworth SR. Tissue factor pathway inhibitor expression in human crescentic glomerulonephritis. *Kidney Int* 1999; **55**: 1311–1318.
6. Ono T, Kanatsu K, Ueda S, *et al.* Detection of the antigenicity of the D-dimer of cross linked fibrin in the glomerulus by plasmin treatment. *Kidney Int* 1994; **46**: 260–265.
7. Holdsworth SR, Thomson NM, Glasgow EF, Atkins RC. The effect of defibrination on macrophage participation in rabbit nephrotoxic nephritis: studies using glomerular culture and electron microscopy. *Clin Exp Immunol* 1979; **37**: 38–43.
8. Ono T, Muso E, Suyama K, *et al.* Intraglomerular deposition of intact cross-linked fibrin in IgA nephropathy and Henoch–Schönlein purpura nephritis. *Nephron* 1996; **74**: 522–528.
9. Mann KG, Jenny RJ, Krishnaswamy S. Cofactor proteins in the assembly and expression of blood clotting enzyme complexes. *Annu Rev Biochem* 1988; **57**: 915–956.
10. Kane WH, Ichinose A, Hagen FS, Davie EW. Cloning of cDNAs coding for the heavy chain region and connecting region of human Factor V, a blood coagulation factor with four types of internal repeats. *Biochemistry* 1987; **26**: 6508–6514.
11. Chiu HC, Schick PK, Colman RW. Biosynthesis of Factor V in isolated guinea pig megakaryocytes. *J Clin Invest* 1985; **75**: 339–346.
12. Gewirtz AM, Keefer M, Doshi K, Annamalai AE, Chiu HC, Colman RW. Biology of human megakaryocyte Factor V. *Blood* 1986; **67**: 1639–1648.
13. Cervený TJ, Fass DN, Mann KG. Synthesis of coagulation Factor V by cultured aortic endothelium. *Blood* 1984; **63**: 1467–1474.
14. Tracy PB, Rohrbach CHMS, Mann KG. Functional prothrombinase assembly on isolated monocytes and lymphocytes. *J Biol Chem* 1983; **258**: 7264–7267.
15. Mazzorana M, Cochrane B, Baffet G, Hubert N, Belleville J, Eloy R. Biosynthesis of Factor V by normal adult rat hepatocytes. *Thromb Res* 1989; **54**: 655–675.
16. Ono T, Liu N, Kasuno K, *et al.* Coagulation process proceeds on cultured human mesangial cells via expression of Factor V. *Kidney Int* 2001; **60**: 1009–1017.
17. Yanase H, Orikasa M, Shimizu F, Kawachi H, Iwanaga T. Immunohistochemical identification of type B intercalated cells in the rat kidney by a monoclonal antibody. *Arch Histol Cytol* 1998; **61**: 151–161.
18. Kihara M, Umemura S, Sugaya T, *et al.* Expression of neuronal nitric oxide synthase and renin in the juxtaglomerular apparatus of angiotensin type-1a receptor gene-knockout mice. *Kidney Int* 1998; **53**: 1585–1593.
19. Kitching AR, Tipping PG, Kurimoto M, Holdsworth SR. IL-18 has IL-12-independent effects in delayed-type hypersensitivity: studies in cell-mediated crescentic glomerulonephritis. *J Immunol* 2000; **165**: 4649–4657.
20. Liu N, Ono T, Suyama K, *et al.* Mesangial Factor V expression colocalized with fibrin deposition in IgA nephropathy. *Kidney Int* 2000; **58**: 598–606.
21. Yang TL, Cui J, Rehumtulla A, *et al.* The structure and function of murine Factor V and its inactivation by protein C. *Blood* 1998; **91**: 4593–4599.
22. Sabath DE, Broome HE, Prystowsky MB. Glyceraldehyde-3-phosphate dehydrogenase mRNA is a major interleukin 2-induced transcript in a cloned T-helper lymphocyte. *Gene* 1990; **91**: 185–191.
23. McLean IW, Nakane PK. Periodate–lysine–paraformaldehyde fixative. A new fixative for immunoelectron microscopy. *J Histochem Cytochem* 1974; **122**: 1077–1083.
24. Ono T, Kanatsu K, Doi T, *et al.* Immunoelectron microscopic localization of fibrin-related antigen in human glomerular diseases. *Nephron* 1989; **52**: 238–243.
25. Hattori T, Shindo S, Hisada T, *et al.* Effects of Onpi-to (TJ-8117) on mesangial injury induced by anti-Thy-1 antibody. *Jpn J Pharmacol* 1995; **105**: 63–75.
26. Alpers CE, Hudkins KL, Gown AM, Johnson RJ. Enhanced expression of 'muscle-specific' actin in glomerulonephritis. *Kidney Int* 1992; **41**: 1134–1142.
27. Kincaid-Smith P. Coagulation and renal disease. *Kidney Int* 1972; **2**: 183–190.
28. Morita T, Suzuki Y, Churg J. Structure and development of the glomerular crescent. *Am J Pathol* 1973; **72**: 349–368.
29. Erlich JH, Holdsworth SR, Tipping PG. Tissue factor initiates glomerular fibrin deposition and promotes major histocompatibility complex class II expression in crescentic glomerulonephritis. *Am J Pathol* 1997; **150**: 873–880.
30. Tipping PG, Holdsworth Sr. The participation of macrophages, glomerular procoagulant activity, and Factor VIII in glomerular fibrin deposition. Studies on anti-GBM antibody-induced glomerulonephritis in rabbits. *Am J Pathol* 1986; **124**: 10–17.
31. Ono T, Liu N, Kasuno K, *et al.* Coagulation process proceeds on cultured human mesangial cells via expression of Factor V. *Kidney Int* 2001; **60**: 1009–1017.
32. Odegaard B, Mann KG. Proteolysis of Factor Va by Factor Xa and activated protein C. *J Biol Chem* 1987; **262**: 11233–11238.
33. Esmon CT. The subunit structure of thrombin-activated Factor V. Isolation of activated Factor V, separation of subunits, and reconstitution of biological activity. *J Biol Chem* 1979; **254**: 964–973.
34. Erlich JH, Apostolopoulos J, Wun TC, Kretzmer KK, Holdsworth SR, Tipping PG. Renal expression of tissue factor pathway inhibitor and evidence for a role in crescentic glomerulonephritis in rabbits. *J Clin Invest* 1996; **98**: 325–335.
35. Heidenreich S, Junker R, Wolters H, *et al.* Outcome of kidney transplantation in patients with inherited thrombophilia: data of a prospective study. *J Am Soc Nephrol* 2003; **14**: 234–239.
36. Imai H, Kodama T, Yasuda T, *et al.* IgA nephropathy associated with mild type-coagulation Factor V deficiency in father and son. *Clin Nephrol* 1995; **44**: 133–134.
37. Floege J, Topley N, Resch K. Regulation of mesangial cell proliferation. *Am J Kidney Dis* 1991; **17**: 673–676.
38. Bolton WK, Innes DJ Jr, Sturgill BC, Kaiser DL. T-cells and macrophages in rapidly progressive glomerulonephritis: clinicopathologic correlations. *Kidney Int* 1987; **32**: 869–876.
39. Neale TJ, Tipping PG, Carson SD, Holdsworth Sr. Participation of cell-mediated immunity in deposition of fibrin in glomerulonephritis. *Lancet* 1988; **2**: 421–424.
40. McHale JF, Harari OA, Marshall D, Haskard DO. Vascular endothelial cell expression of ICAM-1 and VCAM-1 at the onset of eliciting contact hypersensitivity in mice: evidence for a dominant role of TNF- α . *J Immunol* 1999; **162**: 1648–1655.
41. Janssen U, Ostendorf T, Gaertner S, *et al.* Improved survival and amelioration of nephrotoxic nephritis in intercellular adhesion molecule-1 knockout mice. *J Am Soc Nephrol* 1998; **9**: 1805–1814.
42. Lloyd CM, Minto AW, Dorf ME, *et al.* RANTES and monocyte chemoattractant protein-1 (MCP-1) play an important role in the inflammatory phase of crescentic nephritis, but only MCP-1 is involved in crescent formation and interstitial fibrosis. *J Exp Med* 1997; **185**: 1371–1380.
43. Maruyama K, Kashihara N, Yamasaki Y, *et al.* Methylprednisolone accelerates the resolution of glomerulonephritis by sensitizing mesangial cells to apoptosis. *Exp Nephrol* 2001; **9**: 317–326.
44. Ou ZL, Nakayama K, Natori Y, Doi N, Saito T, Natori Y. Effective methylprednisolone dose in experimental crescentic glomerulonephritis. *Am J Kidney Dis* 2001; **37**: 411–417.
45. Yoshikawa N, Ito H, Sakai T, *et al.* A controlled trial of combined therapy for newly diagnosed severe childhood IgA nephropathy. The Japanese Pediatric IgA Nephropathy Treatment Study Group. *J Am Soc Nephrol* 1999; **10**: 101–109.
46. Fujigaki Y, Sun DF, Fujimoto T, *et al.* Mechanisms and kinetics of Bowman's epithelial-myofibroblast transdifferentiation in the formation of glomerular crescents. *Nephron* 2002; **92**: 203–212.

47. Shultz PJ, Knauss TC, Mene P, Abboud HE. Mitogenic signals for thrombin in mesangial cells: regulation of phospholipase C and PDGF genes. *Am J Physiol* 1989; **257**: F366–F374.
48. Monno R, Grandaliano G, Faccio R, *et al.* Activated coagulation Factor X: a novel mitogenic stimulus for human mesangial cells. *J Am Soc Nephrol* 2001; **12**: 891–899.
49. Grandaliano G, Valente AJ, Abboud HE. A novel biologic activity of thrombin: stimulation of monocyte chemotactic protein production. *J Exp Med* 1994; **179**: 1737–1741.
50. Bachli EB, Pech CM, Johnson KM, Johnson DJ, Tuddenham EG, McVey JH. Factor Xa and thrombin, but not Factor VIIa, elicit specific cellular responses in dermal fibroblasts. *J Thromb Haemost* 2003; **1**: 1935–1944.
51. Nomura K, Ono T, Kobayashi I, Liu N, Nogaki E. Effects of factor Xa inhibitor on rat experimental mesangioproliferative glomerulonephritis. *J Am Soc Nephrol* 2002; **13**: 175A (Abstract).

Quantitative trait loci (QTL) analysis reveals a close linkage between the hinge region and trimeric IgA dominance in a high IgA strain (HIGA) of ddY mice

Emi Oida¹, Fumiaki Nogaki¹, Ikei Kobayashi¹, Tadashi Kamata¹, Takahiko Ono¹, Shigeki Miyawaki², Tadao Serikawa³, Haruyoshi Yoshida⁴, Toru Kita¹ and Eri Muso⁵

¹ Department of Cardiovascular Medicine, Kyoto University, Graduate School of Medicine, Kyoto, Japan

² Research Laboratories, Nippon Shinyaku Co. Ltd., Kyoto, Japan

³ Institute of Laboratory Animals, Kyoto University, Graduate School of Medicine, Kyoto, Japan

⁴ Department of Clinical and Laboratory Medicine, Faculty of Medicine, Fukui University, Fukui, Japan

⁵ Department of Nephrology, Kitano Hospital, Tazuke Kofukai Medical Research Institute, Osaka, Japan

Polymerization of IgA has been suggested as one of the causes of mesangial deposition in IgA nephropathy. HIGA mice are an inbred model of IgA nephropathy, established by selective mating of ddY mice. This strain is characterized by a unique profile of the IgA molecule that is dominantly polymeric and has high serum levels with intense IgA deposition on the mesangium. We carried out quantitative trait loci (QTL) analysis, using F2 generations by crossing HIGA with BALB/c mice. Significant linkage of polymeric IgA in serum samples was identified around D12Mit263, which is close to the gene of the immunoglobulin heavy chain on chromosome 12. The amino acid sequence of the α heavy chain revealed marked differences between BALB/c and HIGA mice. Furthermore, most differences were focussed on the hinge region. The DBA/2J strain, which has the same amino acid sequence in the hinge region as the HIGA strain, also showed polymeric IgA dominance but low IgA levels in sera. Size fraction analysis revealed that these polymeric IgA showed trimer dominance in both DBA/2J and HIGA mice. In conclusion, the hinge region plays a key role in trimeric IgA formation in HIGA mice.

Key words: QTL analysis / HIGA strain, trimeric IgA / hinge region

Received	26/2/04
Revised	19/4/04
Accepted	6/5/04

1 Introduction

IgA nephropathy (IgAN) is the most common type of glomerular disease worldwide, and one of the major causes of end-stage renal failure. It presents predominant mesangial deposition of IgA1 [1, 2]. The pathogenesis of IgAN is unknown; however, some immunological disturbances concerned with IgA characters such as higher serum levels, macromolecular size and abnormal glycosylation have been suggested in IgAN [3–5]. Among them, the dominant polymeric IgA, not only in serum but also in the glomerular deposit, was suggested to play a

pathogenic role. For example, circulating polymeric IgA1 was recognized in the sera of 80% of patients with IgAN [6].

Previously, IgAN was not considered as a hereditary disease, although several familial IgA nephropathies were reported [7, 8]. Recently, Gharavi et al. [9] performed a genome-wide linkage analysis in 30 IgAN relatives and demonstrated the linkage of this disease to 6q22-23 with a dominant model of transmission. Although the gene responsible for IgAN remains unclarified, it was expected that the search for the gene that gives rise to polymeric IgA would contribute to the investigation of the pathogenesis of IgAN.

As a murine model of IgA nephropathy, ddY mice were reported to spontaneously develop mesangioproliferative glomerulonephritis with glomerular IgA deposition [10]. These mice show relatively high serum IgA levels with wide individual variation [11]. Recently, an inbred murine model of IgAN, a high IgA strain (HIGA) of ddY

[DOI 10.1002/eji.200425062]

Abbreviations: HIGA mice: A high IgA strain of ddY mice
QTL: Quantitative trait loci **IgAN:** IgA nephropathy **LRS:** Likelihood ratio statistics **LOD:** Logarithm of odds **P/M:** Polymer/monomer ratio

mice, was established by selective mating of high IgA mice from pooled crude ddY mice [12]. HIGA mice show uniformly high IgA levels from a young age, polymeric IgA dominance in the serum and glomerulonephritis with IgA deposition, mimicking human IgAN. In glomerular eluates, dominant dimeric IgA was recognized in these mice [13].

In an attempt to identify the gene related to polymeric IgA, QTL contributing polymeric IgA was mapped using the F2 generation between the HIGA and BALB/c strain, and compared with mapping data concerning the serum level of IgA to investigate the relations between them.

2 Results

2.1 IgA molecular size analysis in F2 by Western blotting

To examine the molecular size of IgA in F2 sera, Western blotting was carried out on samples separated by SDS-PAGE under nonreducing conditions. In the BALB/cA strain, monomeric and dimeric IgA, but no polymeric IgA, were detected. In HIGA mice, large amounts of polymeric IgA were observed. Smaller amounts of dimeric IgA were also detected, but no monomer was visible (Fig. 1A). Since the polymeric IgA formation was still preserved after boiling in SDS and SDS-PAGE, the polymeric IgA of HIGA mice is not constructed through immune complex formation [14]. On the other hand, in F1 sera, the dominant IgA molecule was dimer with small amounts of monomeric IgA and no polymeric IgA was

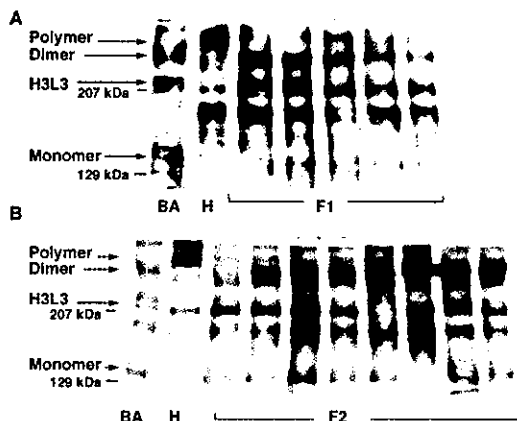


Fig. 1. IgA Western blot analysis in sera. (A) Serum samples of BALB/cA, HIGA and F1 mice were subjected to 6% SDS-PAGE under nonreducing conditions. (B) Serum samples of BALB/cA, HIGA and F2 mice were used. BA, BALB/cA strain; H, HIGA strain. Molecular mass markers (129 and 207 kDa) are shown.

visible (Fig. 1A). In all samples, some of the assembly located around 207 kDa was observed, and it might have been an H3L3 unit according to previous findings [15]. In the F2 generation, IgA molecular size was distributed from monomeric or polymeric dominance (Fig. 1B).

2.2 Linkage analysis

About 600 markers were screened, and 102 microsatellites that clearly showed distinguishable polymorphisms between the BALB/cA and HIGA strains were finally selected. Initially, to investigate the QTL of polymeric IgA, the genotyping of the 102 microsatellite markers located on all chromosomes except Y and the measurement of IgA molecular size were carried out in 84 F2 mice. It was demonstrated that QTL of polymeric IgA was potentially located in chromosome 12. The analysis of the genotype of all 168 F2 mice with regard to polymeric IgA and serum IgA level was also performed in this chromosome. At Mit80, Mit263 and Mit150, significant differences in these phenotypes were found between mice with BALB/c and HIGA genotypes. In addition, the polymer/monomer ratio (P/M) in mice showing the F1 genotype were suppressed compared with those showing the HIGA genotype at these markers, suggesting a recessive transmission (Table 1). In contrast, these markers showed no relation to high IgA ($p=0.889$ at D12Mit263, data not shown). As shown in Fig. 2, D12Mit263 (58.0 cM) provided the greatest logarithm of odds (LOD) score, 15.4 for P/M, whereas for the IgA level these were low and showed no apparent peak. On the other hand, it has been reported that a cluster of immunoglobulin heavy chain genes is located at 58.0 cM (National Center Biotechnology Information; <http://www.ncbi.nlm.nih.gov/>). D12Mit263 was confirmed to be located close to this cluster.

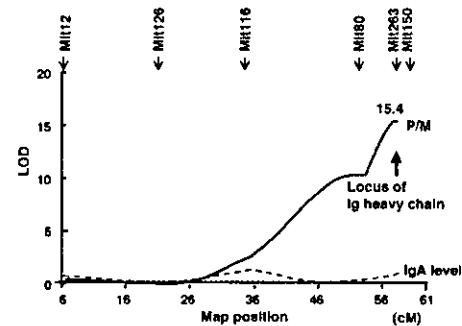


Fig. 2. Map Manager QTX scan of chromosome 12 for P/M, serum IgA level. The location of microsatellite markers used are shown at the top of the figure. The positions of markers were obtained from Mouse Genome Informatics (MGI; <http://www.informatics.jax.org/>). A potential candidate gene of P/M, Ig heavy chain, was located at 58 cM.

Table 1. Correlation between markers on chromosome 12 and P/M

Marker	Map position (cM)	Genotype ^{a)}			<i>p</i> value ^{b)} BALB vs. HIGA
		BALB	HIGA	F1	
Mit12	6.0	5.19±8.98	3.04±5.07	5.38±10.0	0.192
Mit126	22.0	4.38±9.00	3.74±5.78	4.68±8.96	0.728
Mit116	35.0	1.65±1.86	8.69±13.6	4.87±8.24	0.0012
Mit80	53.0	1.25±0.755	12.6±13.6	3.05±5.82	<0.0001
Mit263	58.0	1.23±0.756	14.0±14.4	2.15±1.48	<0.0001
Mit150	59.0	1.24±0.760	13.8±14.2	2.10±1.39	<0.0001

^{a)} The data were obtained from 168 F2 mice. Values are presented as the means ± SD of P/M.

^{b)} *t*-test.

2.3 Comparison of the amino acid sequence of C α among five strains

To examine the possibility that polymeric IgA depends on the amino acid sequence of the α heavy chain, the basic sequences of all three exons in HIGA and BALB/cA mice were determined and translated to amino acids. The comparison of the amino acid sequences revealed 18 amino acid differences throughout C α 1, C α 2 and C α 3, except the tailpiece between BALB/cA and HIGA mice (Fig. 3). The tail-piece cysteine is crucial for dimeric for-

mation of IgA, in addition to polymerization of IgM [16–18]; however, their sequences were identical in the tail-piece. In contrast, most differences were concentrated in the hinge region (8 amino acids). HIGA has one extra Cys residue compared with BALB/cA mice. To investigate the differences in the amino acid sequences in other strains of mice, the α heavy chain in four mouse strains with different IgA allotypes, BALB/cA (Igh-2a), C57BL/6J (Igh-2b), DBA/2J (Igh-2c) and AKR/N (Igh-2d), were compared with the HIGA strain. The sequences of C α of the four strains have been determined and com-



Fig. 3. Differences in the amino acid sequences of the IgA heavy chain from C α 1 to the tailpiece in the BALB/cA and HIGA strains. Asterisks indicate amino acids differing between the BALB/cA and HIGA strains.

Strain	Sequence
AKR	G <u>P</u> <u>P</u> <u>P</u> <u>P</u> <u>C</u> <u>P</u> <u>P</u> <u>*</u> <u>*</u> <u>*</u> <u>*</u> <u>P</u> <u>S</u> <u>C</u> <u>Q</u> <u>P</u>
BALB/cA	G <u>P</u> <u>I</u> <u>P</u> <u>P</u> <u>P</u> <u>P</u> <u>I</u> <u>I</u> <u>I</u> <u>*</u> <u>P</u> <u>S</u> <u>C</u> <u>Q</u> <u>P</u>
C57BL/6J	G <u>P</u> <u>P</u> <u>P</u> <u>P</u> <u>C</u> <u>P</u> <u>P</u> <u>C</u> <u>P</u> <u>*</u> <u>P</u> <u>S</u> <u>C</u> <u>H</u> <u>P</u>
DBA/2J	G <u>I</u> <u>C</u> <u>S</u> <u>P</u> <u>P</u> <u>T</u> <u>T</u> <u>P</u> <u>P</u> <u>P</u> <u>P</u> <u>S</u> <u>C</u> <u>Q</u> <u>P</u>
HIGA	G <u>I</u> <u>C</u> <u>S</u> <u>P</u> <u>P</u> <u>T</u> <u>T</u> <u>P</u> <u>P</u> <u>P</u> <u>P</u> <u>S</u> <u>C</u> <u>Q</u> <u>P</u>

Fig. 4. Comparison of the sequences of the hinge region among HIGA and the other four strains. Asterisks indicate missing amino acids. Amino acids differing from those of the HIGA strain are underlined.

pared [19]: small differences are scattered throughout Cα1, Cα2 and Cα3, but many differences are found in the hinge region. Surprisingly, the hinge sequence of HIGA was very similar to that of DBA/2J (Fig. 4). Since Phillips-Quagliata [19] demonstrated that mouse IgA allotypes have major differences in their hinge region, IgA of HIGA mice might have the same allotype as DBA/2J, Igh-2c.

2.4 Serum IgA molecular size analysis among BALB/cA, C57BL/6J, DBA/2J, AKR/N and HIGA strains

To investigate the linkage between amino acid sequences in the hinge region and the molecular size of serum IgA, Western blotting of serum IgA in these five strains of mice was performed. Samples separated by SDS-PAGE under nonreducing conditions were visualized using the method described above (Fig. 5). Analysis of C57BL/6J showed monomeric and dimeric dominance without polymeric IgA, similar to the pattern in the BALB/cA strain. Polymeric IgA dominance, which is a



Fig. 5. IgA Western blot analysis in sera of five strains. Sera diluted with sample buffer were subjected to 6% SDS-PAGE under nonreducing conditions. H: HIGA strain; D: DBA/2J strain; BL: C57BL/6J strain; BA: BALB/cA strain; A: AKR/N strain. Molecular mass markers (129 and 207 kDa) are shown.

character of the serum of HIGA mice, was also seen in DBA/2J. In the serum of AKR/N, only dimeric IgA was observed and neither polymeric nor monomeric IgA was seen. To reconfirm polymeric IgA dominance in DBA/2J and to investigate the precise molecular size of polymeric IgA, IgA levels in the sera fractionated by HPLC were measured using ELISA (Fig. 6). Polymeric IgA, located between 443 and 669 kDa, was predominant in both HIGA and DBA/2J, while BALB/cA, C57BL/6J and AKR/N showed monomeric and dimeric dominance. Since the size of polymeric IgA was estimated at nearly 500 kDa, polymeric IgA was confirmed to be a trimer. In contrast to the results of Western blotting analysis,

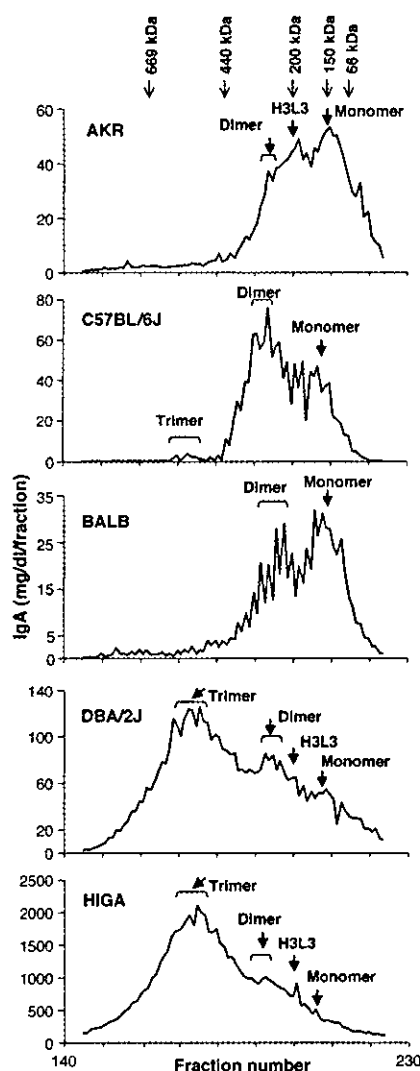


Fig. 6. Size analysis of serum IgA in the AKR/N, C57BL/6J, BALB/cA, DBA/2J and HIGA strains by HPLC. IgA levels of 80 fractions of each sample were measured using ELISA. Molecular masses of marker proteins (in kDa) are shown at the top.

monomeric IgA formed a small peak in both HIGA and DBA/2J, and almost no peak trimer was observed in BALB/cA, C57BL/6J and AKR/N mice.

2.5 Comparison of serum IgA concentrations

To determine the relation between amino acid sequences in the hinge region and serum IgA properties, the serum IgA levels of these four strains possessing different allotypes, BALB/cA, C57BL/6J, DBA/2J and AKR/N, were assessed and compared with those of HIGA mice. While the serum IgA level in HIGA was significantly higher than those of other strains, no significant differences were found among those of the four strains, including DBA/2J mice (Table 2).

2.6 IgA staining of glomeruli

There was mild deposition of IgA in BALB/cA, C57BL/6J and DBA/2J mice, whereas severe deposits were seen in the mesangial areas in HIGA mice (Fig. 7). The results of the quantitative analysis are shown in Table 3. A significant difference was observed only in the HIGA strain.

2.7 Relation between the amount of trimeric IgA and IgA deposition in glomeruli

We selected 43 F2 mice that showed an appearance of polymeric IgA dominance with Western blotting (Fig. 1B); the relation between serum IgA levels and glomerular IgA

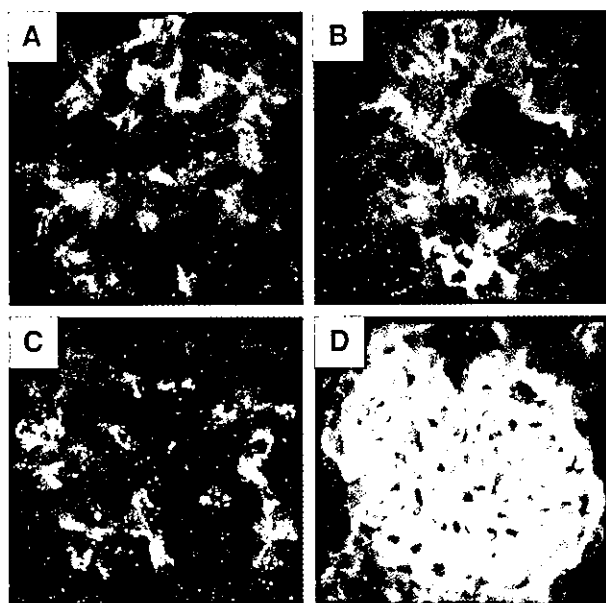


Fig. 7. Immunofluorescence photographs of glomerular IgA deposition in the BALB/cA (A), DBA/2J (B), C57BL/6J (C) and HIGA strains (D) at 30 weeks of age ($\times 400$).

Table 2. Serum IgA levels

Strain	<i>n</i>	Serum IgA level ^{a)} (mg/100 ml)	<i>p</i> value ^{b)} (HIGA vs. other strains)	<i>p</i> value (DBA vs. other strains)
DBA/2J	7	29.41 \pm 21.00	<0.0001	–
AKR/N	3	9.79 \pm 1.83	<0.0001	0.157
BALB/cA	7	25.95 \pm 5.58	<0.0001	0.681
C57BL/6J	7	14.16 \pm 7.32	<0.0001	0.0946
HIGA	7	192.5 \pm 29.82	–	0.0001

^{a)}Values are presented as the means \pm SD of the IgA level.

^{b)} *t*-test.

deposition in them was evaluated by linear regression. As shown in Fig. 8, serum IgA levels were correlated with IgA deposition ($r=0.489$, $p=0.0009$).

3 Discussion

In this study, in HIGA mice, a significant linkage of the trait of trimeric IgA dominance in sera was recognized exclusively with the locus around D12Mit263 on chromosome 12 in a recessive model of transmission with a LOD score of 15.4. On the other hand, D12Mit263 has been reported to be located close to the immunoglobulin heavy chain gene. Analysis of the amino acid sequences of the IgA heavy chain revealed a significant divergence between BALB/cA and HIGA mice (18 amino acids). Most differences were focussed on the hinge region. It was disclosed that the amino acid sequence of this region in the HIGA strain was identical to that in DBA/2J mice. Furthermore, analysis of the molecular size of

Table 3. Analysis of IgA deposition in glomeruli (IgA FITC stain)

Strain	<i>n</i>	Serum IgA deposition degree ^{a)}	<i>p</i> value ^{b)} (HIGA vs. other strains)	<i>p</i> value (DBA vs. other strains)
DBA/2J	7	28.88 \pm 4.06	<0.0001	–
BALB/cA	7	27.85 \pm 3.70	<0.0001	0.681
C57BL/6J	7	30.89 \pm 5.56	<0.0001	0.0946
HIGA	5	192.5 \pm 11.81	–	<0.0001

^{a)}Values are presented as the means \pm SD of the IgA deposition degree, which was expressed numerically using PhotoShop.

^{b)} *t*-test.

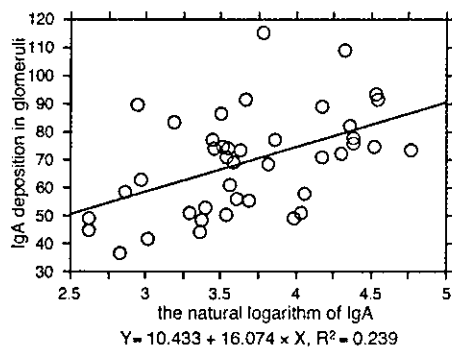


Fig. 8. Correlation between serum IgA levels and IgA deposition in glomeruli in F2 mice, which have polymeric IgA dominance. The grades of IgA deposition were evaluated quantitatively by measuring the intensity of the fluorescence in glomerular areas with PhotoShop 5.0 and graded from 0 to 255.

serum IgA in DBA/2J mice demonstrated the same pattern as HIGA mice with significant trimer IgA dominance. Thus, the amino acid sequence in the hinge region has been clearly shown to play a key role in trimeric IgA dominance in HIGA mice.

No linkage was seen between high serum IgA and the QTL of trimeric IgA dominance. There were two significant QTL of high serum IgA, which were located at chromosomes 2 and 4, respectively (Nogaki et al., submitted). This finding suggests that trimeric IgA formation and the high serum IgA level result from distinct genes in HIGA mice. This is consistent with the serum IgA level not being significantly high in the DBA strain despite trimeric IgA dominance. Although the serum IgA level in original ddY mice varies widely, almost all of them show polymeric IgA dominance [11]. Thus, it is suggested that ddY mice possess the homozygous gene of the IgA hinge, composed of the same sequences as HIGA and DBA mice. Also, the phenotype of polymeric IgA was preserved during the process of establishing HIGA mice, which was performed by selective mating of high AgA mice. Although both HIGA and DBA mice have the same character of molecular size, the linkage between them with regard to pedigree has not been reported previously.

Unexpectedly, the IgA deposition in glomeruli observed in the DBA strain was not significantly higher than those in BALB/cA and C57BL/6J mice. On the other hand, serum IgA levels and IgA deposition in glomeruli in F2 mice, which have polymeric IgA dominance, showed a correlation. Therefore, the trimer of IgA is probably not sufficient by itself for IgA deposition. Other factors, such as high quantity, might be necessary because in HIGA strain the serum IgA level was about seven times higher

than those of other strains. Further investigations for glomerular IgA are currently in progress.

It was unclear which amino acid at the hinge region was responsible for trimeric IgA formation in HIGA and DBA. It is, however, noteworthy that these strains have one extra Cys at the hinge region compared with the BALB/cA strain, while in other regions, no extra Cys are recognized. Within the endoplasmic reticulum, free sulfhydryl groups are oxidized to form disulfide bonds, and almost all cysteine residues in secreted proteins are disulfide bonded [20]. These extra Cys residues are able to form interchain S-S bonds with the J chain or another part of the heavy chain, providing the possibility of forming trimeric IgA. Although AKR/N and C57BL/6J also have extra Cys residues in the hinge region (AKR/N strain has one extra Cys and C57BL/6J has two extra Cys), trimeric IgA was not seen in these strains. This phenomenon could be explained by amino acids flanking the extra Cys residues in those strains. The extra Cys in the hinge region of these mice were surrounded by Pro residues. In human IgA, the major form of IgA2m(1), lacks disulfide bonds between the H and L chain, and it was shown that the presence of Pro in CH1 inhibits the formation of an HL disulfide [20]. Assuming it is possible to extrapolate the mechanism of IgA formation in humans to those in mice, these results suggest that Pro residues adjacent to Cys in AKR/N and C57BL/6J might interfere with trimeric IgA formation.

We demonstrate a new animal model, the DBA/2J strain, which presents trimeric IgA dominance without a high IgA level in the serum. In general, secretory IgA is predominantly polymeric to facilitate efficient transport to the mucosal secretions mediated via the polymeric immunoglobulin receptor (pIgR) [21]. IgA secreted into the gut lumen acts both to protect against viral and bacterial pathogens and for homeostasis of the gut flora [22]. The DBA/2J strain represents a potent tool for clarifying intestinal immunity and for investigating affinity of trimeric IgA for pIgR or sensitivity to pathogens.

Here we have demonstrated that, in the HIGA strain, trimeric IgA formation results from the amino acid sequence in the hinge region. Further genetic analysis of this murine model may facilitate the clarification of the pathogenesis of human IgAN.

4 Materials and methods

4.1 Mice

HIGA mice were bred under specific pathogen-free (SPF) conditions in the Animal Laboratories of Nippon Shinyaku Co. Ltd. (Kyoto, Japan). BALB/cA mice were purchased

from Clea Japan (Tokyo, Japan). By crossing HIGA with BALB/cA mice, F1 (BALB/cA × HIGA) and F2 (F1 × F1) generations were produced and bred at Nippon Shinyaku. All F2 mice ($n=168$) were killed under ether anesthesia at 40 weeks of age, and blood, liver and kidneys were collected. Four strains with different IgA allotypes were investigated: BALB/cA, Igh-2a; C57BL/6J, Igh-2b; DBA/2J, Igh-2c; and AKR/N, Igh-2d. C57BL/6J and DBA/2J mice were obtained from Clea Japan and AKR/N mice were purchased from Japan SLC, Inc. (Shizuoka, Japan). C57BL/6J, DBA/2J, AKR/N, BALB/cA and HIGA mice were killed at 30 weeks of age, and blood, liver and kidneys were collected. All mice used in this study were female. All animal experiments were performed in accordance with institutional guidelines, and the Review Board of Kyoto University approved the ethics of this study.

4.2 IgA staining of renal tissue

Immunofluorescence studies of IgA on frozen renal sections (3 μm) were performed as described previously [10]. The grades of deposition were evaluated quantitatively by measuring the intensity of the fluorescence in glomerular areas with PhotoShop 5.0 (Adobe, San Jose, CA) and graded from 0 to 255 [14]. Five randomly selected glomeruli in each F2 mouse and ten glomeruli in each BALB/cA, C57BL/6J, DBA/2J and HIGA mouse were measured and the mean value of the grades was used for analysis.

4.3 ELISA

Total IgA in the sera was measured using a modification of the sandwich ELISA described previously [23]. Briefly, microtitration plates (Corning, Cambridge, MA) were coated with goat anti-mouse IgA antibodies (Cappel Laboratories, Cochranville, PA) and blocked with BSA. After incubation with the serum samples, alkaline-phosphatase (ALP)-conjugated goat anti-mouse IgA antibody (Zymed Laboratories, South San Francisco, CA) was applied. The plates were washed, and developed using *p*-nitrophenyl phosphate (Sigma, St. Louis, MO) as an ALP substrate. Absorbance was measured using an ELISA reader.

4.4 Western blot analysis

The IgA molecular size in sera was examined by Western blot analysis under nonreducing conditions, in 30- or 40-week-old mice, as described previously [24]. The samples were diluted with sample buffer which contained 0.05 M Tris-HCl (pH 6.8), 2% SDS, 10% glycerol, and 0.1% bromophenol blue, and boiled for 1 min. The samples were run on 6% SDS-polyacrylamide gels with molecular mass markers (129 and 207 kDa, Bio-Rad, Hercules, CA) in a Bio-Rad mini-protean II gel electrophoresis apparatus at 30 mA for 2.5 h. The gels were then blotted onto a polyvinylidene difluoride membrane (Amersham, Little Chalfont, GB) at 100 V

for 3.5 h. Different forms of IgA were analyzed using rabbit anti-mouse IgA (Zymed Laboratories), followed by goat horseradish peroxidase-conjugated anti-rabbit-IgG (BioSource, Camarillo, CA). The membrane was then drenched in ECL reagent (Amersham) and exposed to ECL hyperfilm (Amersham) for 10 s. Signal intensity was measured using the NIH Image and then the IgA molecular size was expressed as polymer/monomer ratios (P/M).

4.5 HPLC

Size fractionation of the pooled sera was performed by HPLC on a 7.5 mm × 60 cm SW column (5–1,000-kDa fractionation range; Tosoh, Tokyo, Japan) with a flow rate of 0.5 ml/min. Eighty fractions of each sample were collected in 0.1 M phosphate buffer, pH 7.0, containing 0.1 M NaCl. A molecular weight marker kit for gel filtration chromatography (Sigma) was used as a molecular mass marker. IgA levels of the samples were measured using ELISA.

4.6 Genotyping of microsatellite markers

Genomic DNA was extracted from the liver by the standard chloroform/phenol method. SSLP primers were purchased from Research Genetics (Huntsville, AL) or DNA composition companies. Polymorphisms of microsatellite markers were detected as previously described with slight modification [25]. A reaction volume of 20 μl containing 0.2 mM dNTP, 2 μl of 10× Ex Taq buffer, 0.5 μM SSLP primers, 0.5 U TaKaRa Ex Taq (Takara Bio. Inc., Shiga, Japan) and 80 ng genomic DNA was prepared for PCR in 96-well plates. After 5 min incubation at 94°C, the reactions were amplified through 40 cycles of 45 s at 94°C, 45 s at 55°C, 1 min at 72°C, followed by 7 min at 72°C. Detection of PCR products was performed by loading on 5% agarose gels (Invitrogen, Carlsbad, CA).

4.7 Linkage analysis

First, the genotyping of microsatellites in all chromosomes, except the Y chromosome, and the measurement of the IgA molecular size in 84 F2 mice was performed. Initial determinations of statistical differences were obtained by an unpaired *t*-test. For QTL analysis, Map Manager QTX software version 0.23 was used [26]. The significance of each potential association was measured using the likelihood ratio statistics (LRS). LRS were converted into the logarithm of odds (LOD) by dividing by 4.61. A significant LOD score was above the recommended threshold value of 4.3 [27]. After the chromosome in which QTL of polymeric IgA were potentially located was identified, all 168 F2 mice in this chromosome were analyzed.

Table 4. PCR primers for DNA sequences

Primer name	Sequence (5'-3')
Ca1 forward	TGGGCAGTGTGAAGACTACT
Ca1 reverse	TTCTCCTTTGCTGTCCCCTT
Ca2 forward	AGGAATCCCTCAGAAACCTC
Ca2 reverse	TCAGACAAGGAGAGCAAGAC
Ca3 forward	ATCACAGAGGGAAATTGGAG
Ca3 reverse	GCAGGGATACTTTGGATGAG

4.8 DNA sequences

DNA sequences of a constant lesion in the IgA heavy chain (Ca1, Ca2, Ca3 and tailpiece) of three allotypes (Igh-2b, Igh-2c and Igh-2d) were retrieved from GenBank (acc. no. AY045741–AY045752). To examine DNA sequences in HIGA and BALB/cA mice, primers were designed from the introns which were located around the Ca1, Ca2 and Ca3 (Table 4). PCR was then performed using genomic DNA of HIGA and BALB/cA mice, respectively. The amplified fragments were sequenced by TaKaRa Bio. Inc. DNA sequences were translated to amino acids using GENETYX-MAC Ver. 11.0.

4.9 Statistical analysis

In the analyses of F2 mice, determinations of statistical differences between BALB/c and HIGA genotypes were assessed using the unpaired *t*-test with StatView software version 5.0. Differences in serum IgA levels among inbred strains were also analyzed by the unpaired *t*-test. The results are expressed as means \pm SD. Differences were considered significant at $p < 0.05$.

Acknowledgements: The authors thank Ms. Yukiko Ano, Ms. Rie Hikawa and Ms. Yurika Sueno for their technical assistance. This work was supported by a grant-in-aid for General Scientific Research from the Japanese Ministry of Education, Culture, Sports, Science and Technology, and by a grant from the Study Group on IgA Nephropathy.

References

- 1 Julian, B. A., Waldo, F. B., Rifai, A. and Mestecky, J., IgA nephropathy, the most common glomerulonephritis worldwide. A neglected disease in the United States? *Am. J. Med.* 1988. **84**: 129–132.
- 2 Chauveau, D. and Droz, D., Follow-up evaluation of the first patients with IgA nephropathy described at Necker Hospital. *Contrib. Nephrol.* 1993. **104**: 1–5.
- 3 Woodroffe, A. J., Gormly, A. A., McKenzie, P. E., Wootton, A. M., Thompson, A. J., Seymour, A. E. and Clarkson, A. R., Immunologic studies in IgA nephropathy. *Kidney Int.* 1980. **18**: 366–374.
- 4 Monteiro, R. C., Halbwachs-Mecarelli, L., Roque-Barreira, M. C., Noel, L. H., Berger, J. and Lesavre, P., Charge and size of mesangial IgA in IgA nephropathy. *Kidney Int.* 1985. **28**: 666–671.
- 5 Mestecky, J., Tomana, M., Crowley-Nowick, P. A., Moldoveanu, Z., Julian, B. A. and Jackson, S., Defective galactosylation and clearance of IgA1 molecules as a possible etiopathogenic factor in IgA nephropathy. *Contrib. Nephrol.* 1993. **104**: 172–182.
- 6 Valentijn, R. M., Radl, J., Haaijman, J. J., Vermeer, B. J., Weening, J. J., Kauffmann, R. H., Daha, M. R. and van Es, L. A., Circulating and mesangial secretory component-binding IgA-1 in primary IgA nephropathy. *Kidney Int.* 1984. **26**: 760–766.
- 7 Julian, B. A., Quiggins, P. A., Thompson, J. S., Woodford, S. Y., Gleason, K. and Wyatt, R. J., Familial IgA nephropathy. Evidence of an inherited mechanism of disease. *N. Engl. J. Med.* 1985. **312**: 202–208.
- 8 Julian, B. A., Woodford, S. Y., Baehler, R. W., McMorro, R. G. and Wyatt, R. J., Familial clustering and immunogenetic aspects of IgA nephropathy. *Am. J. Kidney Dis.* 1988. **12**: 366–370.
- 9 Gharavi, A. G., Yan, Y., Scolari, F., Schena, F. P., Frasca, G. M., Ghiggeri, G. M., Cooper, K., Amoroso, A., Viola, B. F., Battini, G., Caridi, G., Canova, C., Farhi, A., Subramanian, V., Nelson-Williams, C., Woodford, S., Julian, B. A., Wyatt, R. J. and Lifton, R. P., IgA nephropathy, the most common cause of glomerulonephritis, is linked to 6q22–23. *Nat. Genet.* 2000. **26**: 354–357.
- 10 Imai, H., Nakamoto, Y., Asakura, K., Miki, K., Yasuda, T. and Miura, A. B., Spontaneous glomerular IgA deposition in ddY mice: an animal model of IgA nephritis. *Kidney Int.* 1985. **27**: 756–761.
- 11 Muso, E., Yoshida, H., Takeuchi, E., Shimada, T., Yashiro, M., Sugiyama, T. and Kawai, C., Pathogenic role of polyclonal and polymeric IgA in a murine model of mesangial proliferative glomerulonephritis with IgA deposition. *Clin. Exp. Immunol.* 1991. **84**: 459–465.
- 12 Miyawaki, S., Muso, E., Takeuchi, E., Matsushima, H., Shibata, Y., Sasayama, S. and Yoshida, H., Selective breeding for high serum IgA levels from noninbred ddY mice: isolation of a strain with an early onset of glomerular IgA deposition. *Nephron* 1997. **76**: 201–207.
- 13 Muso, E., Yoshida, H., Takeuchi, E., Yashiro, M., Matsushima, H., Oyama, A., Suyama, K., Kawamura, T., Kamata, T., Miyawaki, S., Izui, S. and Sasayama, S., Enhanced production of glomerular extracellular matrix in a new mouse strain of high serum IgA ddY mice. *Kidney Int.* 1996. **50**: 1946–1957.
- 14 Kessler, S. W., Rapid isolation of antigens from cells with a staphylococcal protein A-antibody adsorbent: parameters of the interaction of antibody-antigen complexes with protein A. *J. Immunol.* 1975. **115**: 1617–1624.
- 15 Sorensen, V., Rasmussen, I. B., Norderhaug, L., Natvig, I., Michaelsen, T. E. and Sandlie, I., Effect of the IgM and IgA secretory tailpieces on polymerization and secretion of IgM and IgA. *J. Immunol.* 1996. **156**: 2858–2865.
- 16 Atkin, J. D., Pleass, R. J., Owens, R. J. and Woof, J. M., Mutagenesis of the human IgA1 heavy chain tailpiece that prevents dimer assembly. *J. Immunol.* 1996. **157**: 156–159.
- 17 Davis, A. C., Roux, K. H. and Shulman, M. J., On the structure of polymeric IgM. *Eur. J. Immunol.* 1988. **18**: 1001–1008.
- 18 Sitia, R., Neuberger, M., Alberini, C., Bet, P., Fra, A., Valetti, C., Williams, G. and Milstein, C., Developmental regulation of IgM secretion: the role of the carboxy-terminal cysteine. *Cell* 1990. **60**: 781–790.

- 19 Phillips-Quagliata, J. M., Mouse IgA allotypes have major differences in their hinge regions. *Immunogenetics* 2002. **53**: 1033–1038.
- 20 Chintalacheruvu, K. R., Yu, L. J., Bhola, N., Kobayashi, K., Fernandez, C. Z. and Morrison, S. L., Cysteine residues required for the attachment of the light chain in human IgA2. *J. Immunol.* 2002. **169**: 5072–5077.
- 21 Kamata, T., Nogaki, F., Fagarasan, S., Sakiyama, T., Kobayashi, I., Miyawaki, S., Ikuta, K., Muso, E., Yoshida, H., Sasayama, S. and Honjo, T., Increased frequency of surface IgA-positive plasma cells in the intestinal lamina propria and decreased IgA excretion in hyper IgA (HIGA) mice, a murine model of IgA nephropathy with hyper IgA. *J. Immunol.* 2000. **165**: 1387–1394.
- 22 Fagarasan, S. and Honjo, T., Intestinal IgA synthesis: regulation of front-line body defences. *Nat. Rev. Immunol.* 2003. **3**: 63–72.
- 23 Nogaki, F., Muso, E., Kobayashi, I., Kusano, H., Shirakawa, K., Kamata, T., Oyama, A., Ono, T., Miyawaki, S., Yoshida, H. and Sasayama, S., Interleukin 12 induces crescentic glomerular lesions in a high IgA strain of ddY mice, independently of changes in IgA deposition. *Nephrol. Dial. Transplant.* 2000. **15**: 1146–1154.
- 24 Hendrickson, B. A., Conner, D. A., Ladd, D. J., Kendall, D., Casanova, J. E., Corthesy, B., Max, E. E., Neutra, M. R., Seidman, C. E. and Seidman, J. G., Altered hepatic transport of immunoglobulin A in mice lacking the J chain. *J. Exp. Med.* 1995. **182**: 1905–1911.
- 25 Shimizu, M., Higuchi, K., Bennett, B., Xia, C., Tsuboyama, T., Kasai, S., Chiba, T., Fujisawa, H., Kogishi, K., Kitado, H., Kimoto, M., Takeda, N., Matsushita, M., Okumura, H., Serikawa, T., Nakamura, T., Johnson, T. E. and Hosokawa, M., Identification of peak bone mass QTL in a spontaneously osteoporotic mouse strain. *Mamm. Genome* 1999. **10**: 81–87.
- 26 Manly, K. F., Cudmore, R. H., Jr. and Meer, J. M., Map Manager QTX, cross-platform software for genetic mapping. *Mamm. Genome* 2001. **12**: 930–932.
- 27 Lander, E. and Kruglyak, L., Genetic dissection of complex traits: guidelines for interpreting and reporting linkage results. *Nat. Genet.* 1995. **11**: 241–247.

Correspondence: Eri Muso, Department of Nephrology, Kitano Hospital, Tazuke Kofukai Medical Research Institute, 20-4-2, Ogimachi, Kita-Ku, Osaka, 530-8480, Japan
Fax: +81-6-6312-8867
e-mail: muso@kitano-hp.or.jp

PAPER

Expression and activity analyses of CTLA4 in peripheral blood lymphocytes in systemic lupus erythematosus patients

M Hirashima^{1*}, T Fukazawa¹, K Abe¹, Y Morita¹, M Kusaoi¹ and H Hashimoto¹
Department of Internal Medicine and Rheumatology, Juntendo University School of Medicine, Tokyo, Japan

The objective of this study was to determine the expression and activity of CTLA4 in T-cells of systemic lupus erythematosus (SLE) patients. Expression of CTLA4 on freshly isolated peripheral blood T-cells was evaluated in 33 SLE patients and 25 controls using flow cytometry. The T-cells from 19 SLE patients and 22 controls were stimulated and cultured with Chinese hamster ovary cells expressing CD80 (CHO-CD80) or with CHO cells. T-cell proliferation was determined with [³H] thymidine incorporation (CPM), and the inhibitory effect of CTLA4 on T-cell proliferation was evaluated by the ratio of CPM for T-cells with CHO-CD80 cells to that of T-cells with CHO cells (the CHO-CD80/CHO ratio). Intracellular CTLA4 expression in freshly isolated peripheral blood T-cells was significantly higher in SLE patients than the controls ($P < 0.05$), but there was no correlation with clinical features or disease activity. The CHO-CD80/CHO ratio of SLE patients was significantly higher than that of the controls ($P < 0.05$). Among SLE patients, the CHO-CD80/CHO ratio of patients with lupus nephritis was significantly higher than that of patients without lupus nephritis ($P < 0.05$). In conclusion, our data suggest that CTLA4 expression is not impaired in SLE patients, but there is a possibility of decreased inhibitory effect of CTLA4 involved in the pathogenesis of SLE. *Lupus* (2004) 13, 24–31.

Key words: CTLA4; lupus nephritis; systemic lupus erythematosus

Introduction

T-cell activation requires at least two signals. The first is the interaction between antigen-specific T-cell receptors and the antigen major histocompatibility complex (MHC). The other is the co-stimulatory signal. Cytotoxic T-lymphocyte-associated antigen-4 (CTLA4) and CD28, which are co-stimulatory molecules on T-cells, bind with the same ligands of CD80 and CD86 on antigen-presenting cells (APCs) and cooperatively regulate T-cell activation. CTLA4 is a T-cell membrane receptor homologous to CD28, but whose function is different from CD28. CD28 is expressed constitutively on T-cells, whereas CTLA4 is expressed transiently only on activated T cells. CTLA4 is localized predominantly within the intracellular compartments and its expression level on the cell surface is only a small fraction in comparison to that of CD28 after T-cell activation. This cell surface expression is rapidly internalized through clathrin-

mediated endocytosis and accumulates within the endosomes of activated T-cells. CTLA4 binds with CD80 and CD86 as well as CD28 but with a 20- to 50-fold greater affinity. A function of CTLA4 is in the termination of immune responses by delivering a negative regulatory signal, whereas CD28 provides a critical co-stimulatory signal essential for the initiation and progression of T-cell immunity.^{1–5}

A lack or modification of negative signals through CTLA4 in mice is implicated in autoimmune diseases. CTLA4-deficient mice are known to develop lymphoproliferative syndromes and autoimmune diseases.⁶ In experimental autoimmune encephalomyelitis murine models, anti-CTLA4 treatment resulted in increased severity of disease activity and higher incidences of relapse.^{1,7,8} Thus, CTLA4 plays an essential role in the prevention of uncontrolled T-cell activation. In addition, *CTLA4* gene polymorphisms have been known to exist in patients with Graves' disease,⁹ autoimmune diabetes mellitus,^{10,11} multiple sclerosis¹² and rheumatoid arthritis.¹³ Together with these findings, it is suggestive that CTLA4-CD80/CD86 interaction plays a critical role in regulating self-tolerance, and in the susceptibility to autoimmune diseases.

*Correspondence: Mika Hirashima, Department of Internal Medicine and Rheumatology, Juntendo University School of Medicine, 2-1-1 Hongo, Bunkyo-Ku, Tokyo 113-8421, Japan. E-mail: jmika@med.juntendo.ac.jp
Received 27 February 2003; accepted 20 August 2003

Systemic lupus erythematosus (SLE) is an autoimmune disorder that includes abnormalities of T-lymphocytes, as well as hyper-reactive B-cells that produce autoantibodies. Peripheral blood lymphocytes from patients with SLE often contain activated T-cells¹⁴⁻¹⁶ and auto-reactive T-cells are postulated to be involved in a major role in the pathogenesis of SLE. One possible explanation for these abnormal activations in lupus lymphocytes is the lack or modification in the auto-reactive elimination of activated T-cells that respond to foreign antigens and in clonal deletion of auto-reactive T-cells in the periphery. Hyper-activities of both B- and T-lymphocytes in SLE are frequently observed, but no studies have investigated the expression of CTLA4 in relation to the clinical feature and activity of SLE and the function of CTLA4.

The aim of this study is to investigate and evaluate the impaired expression and activity of CTLA4 molecules in SLE patients. First, CTLA4 expression in peripheral blood T-cells and its relation to clinical

features and activities were investigated. Next, the inhibitory activity of CTLA4 on T-cell proliferation was investigated and evaluated.

Patients and methods

Patients and control subjects

Lymphocyte marker analysis was performed in 33 SLE patients (32 females and one male, age: 15-70 years, with mean of 33.3 years) (Table 1), who were diagnosed according to the American College of Rheumatology Criteria¹⁷ and 25 age-matched healthy subjects as the controls. The SLE Disease Activity Index (SLEDAI) score¹⁸ for each patient was determined. Patients were selected from patients receiving steroid therapy only in order to avoid bias related to immunosuppressive drugs. Data on age, sex, duration of disease, SLEDAI, type of organ involvement, dosage of prednisolone (at time

Table 1 Characteristics of the SLE patients enrolled in the study for immunofluorescence analysis of lymphocytes

Patient	Years of SLE	Sex	Age (years)	SLEDAI	Organ involvement	Prednisolone (mg/day)	CD28* CTLA4 (%) ^a
1	24	F	44	2	GN	7	14.91
2	10	M	43	32	GN, Se, TH	60	13.12
3	2	F	23	1	TH	15	9.32
4	0.1	F	24	24	CNS	0	8.48
5	14	F	32	18	GN	20	8.08
6	5	F	28	12	GN	20	7.80
7	7	F	41	6	Hepa	10	6.67
8	3	F	20	16	GN	60	6.64
9	7	F	29	18	CNS, E	10	5.94
10	22	F	40	16	GN	10	4.27
11	7	F	24	3	None	35	4.02
12	9	F	49	27	GN,Se	0	4.00
13	3	F	46	2	HA	12.5	3.30
14	1	F	21	3	TH	0	2.93
15	29	F	53	10	GN	7.5	2.51
16	8	F	27	18	TH	10	2.43
17	8	F	26	9	GN	25	2.28
18	1.3	F	48	6	GN, TH, CNS	22.5	2.25
19	2	F	15	16	GN	17.5	1.97
20	9	F	47	14	GN	30	1.78
21	0.7	F	32	11	GN,E	0	1.75
22	7	F	19	6	GN	12.5	1.67
23	0.3	F	15	9	Se, GN, CNS	80	1.60
24	0.1	F	20	8	Se, HA, GN	10	1.46
25	5	F	44	12	GN	30	1.45
26	0.3	F	39	2	TH	45	1.38
27	0.2	F	43	34	GN, TH	0	1.04
28	26	F	70	1	None	5	1.00
29	1.5	F	25	47	CNS, GN	15	0.96
30	0.2	F	54	4	Cys	0	0.89
31	5	F	16	26	CNS, GN	80	0.81
32	0.7	F	18	4	HA, TH, E	45	0.71
33	0.1	F	25	16	GN	30	0.28

SLEDAI = SLE Disease Activity Index; CNS = central nervous systems; GN = glomerulonephritis; Cys = lupus cystitis; Se = serositis; E = lupus exanthem; TH = thrombocytopenia; Hepa = lupus hepatitis; HA = hemolytic anemia; None = no organ involvement.

*Intracellular CTLA4 expression in freshly isolated peripheral CD28 positive T-cells.

Based on two-colour flow cytometry, intracellular CTLA4 expression in-freshly isolated peripheral CD28 positive T-cells (%) was investigated.

of hematological analysis) are shown in Table 1. T-cell proliferation analysis was performed in 19 SLE patients (17 females and two males, age: 16–70 years with mean of 38.1 years) (Table 2) and 22 age-matched controls.

Monoclonal antibodies (MAbs)

The following MAbs were used in this study: phycoerythrin (PE)-labeled anti-human CTLA-4 (BNI3.1, Mouse IgG2a, PharMingen, San Diego, CA), PE-labeled anti-mouse IgG2a as the isotype control, fluorescein isothiocyanate (FITC)-labeled anti-CD28 (KOLT-2, Mouse IgG1, PharMingen).

Cells

Peripheral blood mononuclear cells (PBMCs) were isolated from heparinized blood of SLE patients and controls by Ficoll–Hypaque density-gradient centrifugation (Muto Pure Chemicals, Tokyo, Japan). After three washings with 0.1% fetal calf serum (FCS) with phosphate-buffered saline (PBS), the cells were resuspended in RPMI1640 (Nissui Pharmaceutical, Tokyo, Japan) containing 10% FCS. These cells were used for immunofluorescence staining by FACStar plus flow cytometry (Becton Dickinson, San Jose, CA) and for T-cell proliferation analysis.

Transfectants

Human CD80 cDNA was cloned by PCR and the sequence was confirmed with the DNA sequencer. The cDNA was then subcloned into the expression vector pDNA3.1 (Invitrogen, San Diego, CA). This construct was transfected by lipofectamin plus (Invitrogen, San Diego, CA) into the Chinese hamster ovary (CHO) cells and then cultured with 500 µg/mL of G418; viable cells remaining after culture were selected for the study analyses. CD80-expressing cells were cloned by limiting dilution, and CD80 expression was confirmed by FACScan.

Immunofluorescence analysis of lymphocytes

Intracellular detection of CTLA4 was performed according to the direct intracellular immunofluorescence procedure (Becton Dickinson). PBMCs were stained immediately after isolation and the cells were stained with the FITC-labeled anti-CD28 antibody. After surface staining, the red blood cells were lysed by adding the lysing solution (Cat. No. 349202). Cell mixture was vortexed and incubated for 10 minutes at room temperature followed by centrifugation at 500 g for five minutes. Permeabilizing solution (Cat. No. 340457) was then added to the cells and incubated for

10 minutes at room temperature in the absence of light. After washing with PBS containing 0.5% FCS, PE-labeled anti-human CTLA4 antibody or PE-labeled anti-mouse IgG2a as the isotype control was added and incubated at room temperature in the absence of light. The cells were resuspended in 1% paraformaldehyde in PBS after washing. The cells were analysed by FACStar plus flow cytometry.

T-cell purification

T-cells were purified from PBMCs using the CD4 and CD8 positive isolation kit (DYNAL, Oslo, Norway). Briefly, CD4 and CD8 Dynabeads were added to the PBMCs (beads: PBMCs ratio 2:1) and incubated with rotation at 4°C for 30 minutes. The beads bound isolated cells were washed four to five times in RPMI1640/10%FCS using the Dynal magnetic device. To obtain CD4 and CD8 positive T-cells from the beads, DETACHaBEAD CD4/CD8 was added to the cell suspension and incubated with rotation at room temperature for 60 minutes and the cells detached from beads were collected. This selection procedure routinely yielded preparations of 80–90% of CD4 and CD8 positive cells, as confirmed with the flow FACStar plus flow cytometry.

T-cell proliferation assays

Proliferation assays were performed in triplicate in 96-well plates with a final volume of 200 µl per well in RPMI1640/10% FCS and antibiotics as previously described.¹⁹ T-cells (5×10^4) were cultured with a combination of PMA, ionomycin (PI) with CHO or CHO-CD80 cells fixed with the addition of paraformaldehyde at a CHO:T cell ratio of 2:1. Cell mixtures were incubated at 37°C for three days, and then incubated for six hours with the addition of 1 µCi [³H] thymidine per well. Cells were harvested with 96-well filter plates using a Packard (Meriden, CT) 96-well harvester, and [³H] thymidine uptake was determined via liquid scintillation counting. In procedures where blocking Abs were used, CTLA4Ig (Genzyme Techno #2325) or isotype-matched mouse Ig was added at commencement of culture. Data were plotted as mean values determined in triplicate.

Statistical analysis

Student's *t*-test was used to evaluate the group means of continuous variables. *P*-values of less than 0.05 were considered statistically significant.

Table 2 Characteristics of the SLE patients enrolled in the study for T-cell proliferation assays

Patient	Sex	Age (years)	SLEDAI	Organ involvement	Prednisolone (mg/day)	CHO-CD80/CHO*
1	F	21	12	GN, CNS	80	0.453
2	F	28	10	CNS, TH	60	0.634
3	F	32	16	GN, HA	30	0.766
4	F	25	18	GN, HA	80	0.719
5	F	17	6	CNS, GN, TH	27	0.860
6	F	54	4	Cys	0	0.355
7	F	56	4	CNS, Se	80	0.607
8	F	70	1	None	5	0.318
9	M	37	14	GN, Se	50	1.296
10	F	49	13	GN, TH	22	1.054
11	F	55	10	None	30	0.345
12	M	38	12	GN	25	0.538
13	F	33	12	GN	45	1.163
14	F	38	8	GN	30	1.050
15	F	29	12	GN	10	0.710
16	F	16	16	GN	18	0.630
17	F	64	4	IP	5	0.470
18	F	38	4	None	10	0.879
19	F	24	4	None	8	0.759

SLEDAI = SLE Disease Activity Index; CNS = central nervous system; GN = glomerulonephritis; Cys = lupus cystitis; Se = serositis; TH = thrombocytopenia; HA = hemolytic anemia; IP = interstitial pneumonia; None = no organ involvement.

*The ratio of CPM for T-cells with CHO-CD80 cells so that of T-cells with CHO cells. An increase in this ratio reflects the amount of impairment of T-cell proliferation by CTLA4.

Results

Comparison of CTLA4 expression in peripheral CD28 positive T-cells in SLE patients and controls

CTLA4 expression is restricted to the subset of T-cells that also expresses cell surface CD28 and cooperatively regulates T-cell activation by CD80/CD86.^{20,21} Therefore, CTLA4 expression on freshly isolated peripheral blood CD28 positive T-cells was evaluated. Detection of cell surface CTLA4 expression on CD28 positive T-cells was minimal and was significantly less than that of the intracellular CTLA4 ($P < 0.01$) in all SLE patients and controls (Table 3). Since CTLA4 expression was up-regulated after stimulation, we evaluated the kinetics of cell surface and intracellular CTLA4 expression. After PI stimulation, surface and intracellular expressions of CTLA4 in CD28 positive T-cells were up-regulated, with peak levels achieved between 48 and 72 hours. The kinetics were similar in the controls and SLE patients. The kinetics of cell surface CTLA4 expression paralleled the kinetics of intracellular CTLA4 (data not shown). This data coincided with previous reports in mice.²² For this reason, we compared the intracellular expression of CTLA4 in freshly isolated CD28 positive T-cells obtained from 33 SLE patients (Table 1) and 25 controls. The percentage of intracellular CTLA4 expression in CD28 positive T-cells was significantly greater in SLE patients than in the controls ($P < 0.05$). The distribution in the percentage of individual intracellular CTLA4 expression in CD28 positive

T-cells is shown in Figure 1 and intracellular CTLA4 expression in CD28 positive T-cells in each individual SLE patient is tabulated in Table 1.

No association of SLE clinical features and intracellular CTLA4 expression

Intracellular CTLA4 expression in CD28 positive T-cells (Table 1) did not reveal any correlation with clinical features and disease activities such as anti-DNA antibody titer, low complement and SLEDAI score (data not shown).

Analysis of the negative regulatory function of CTLA4 on T-cell proliferation mediated by CD80 in SLE patients

CTLA4 has been described as a physiologic inhibitor of T-cell activation. To determine whether CTLA4 functions adequately in SLE patients, we evaluated

Table 3 Comparison of CTLA4 expression in peripheral CD28 positive T-cells in SLE patients and controls

	CTLA4 expression on CD28 ⁺ T-cells (mean \pm SEM)		P
	Cell surface	Intracellular	
Controls ($n = 25$)	0.174 \pm 0.166	1.990 \pm 1.426	< 0.001
SLE ($n = 34$)	0.299 \pm 0.445	3.870 \pm 3.657	< 0.001
P	0.189	< 0.05	

Values are expressed as mean \pm SD. P-values were determined with the student's *t*-test.

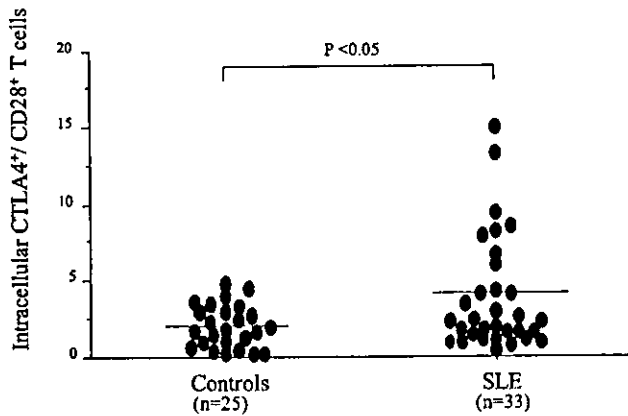


Figure 1 Intracellular CTLA4 expression in freshly isolated peripheral CD28 positive T-cells in SLE patients and controls (median values are indicated by the horizontal bar; *P*-values were determined with the student's *t*-test).

its function by T-cell proliferation assay inhibited by CD80 in a CTLA4-dependent manner.¹⁹ Purified T-cells from SLE patients and controls were cultured with a combination of PMA, ionomycin (PI) with CHO or CHO-CD80 cells fixed with paraformaldehyde. Substantial T-cell proliferation occurred in T-cells from both SLE patients and controls when T-cells were cultured with PI stimulation alone or PI plus CHO cells. When CHO-CD80 cells were added to the T-cells treated with PI, a negative effect on T-cell proliferation was demonstrated (Figure 2). These experiments demonstrated that the inhibition of PI-induced T-cell proliferation is dependent on CD80. Because CD80 can potentially interact with both CD28 and CTLA4, our findings suggested the possibility that CD80 may be involved in the role to

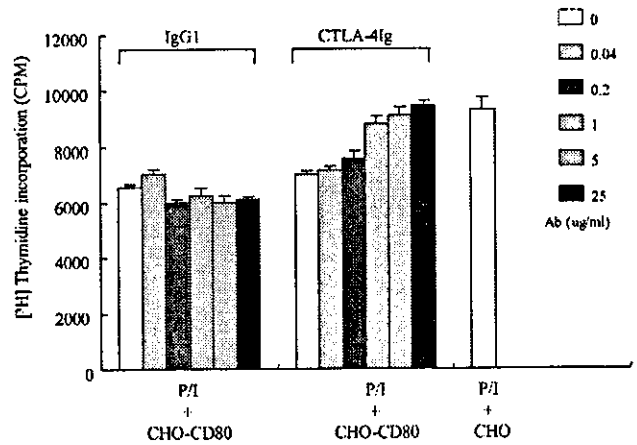


Figure 3 Effect of CTLA4Ig. Purified T-cells from the control were stimulated as in previous experiments with PI in the presence of either CHO cells or CHO-CD80 transfectants. CTLA4Ig or control IgG1 was present at 0, 0.04, 0.2, 1, 5 and 25 µg/mL from commencement of culture. After three days of culture, proliferation analysis was conducted with [³H] thymidine incorporation.

inhibit responses via both CTLA4 and CD80. To confirm that the CD80-mediated inhibition was predominantly via CTLA4, we performed dose-dependent titration experiments of CTLA4Ig and compared the results with that of the control IgG1. The results revealed that in purified T-cells from the controls were demonstrated substantial increases in T-cell proliferation to PI in the presence of CTLA4Ig but not in the presence of the control IgG1. This increase by CTLA4Ig demonstrated a dose-dependent response (Figure 3). This result demonstrated that the CD80-mediated inhibition was predominantly via CTLA4 and was consistent with another study.¹⁹ SLE T-cells are known to be depressed *in vitro* response

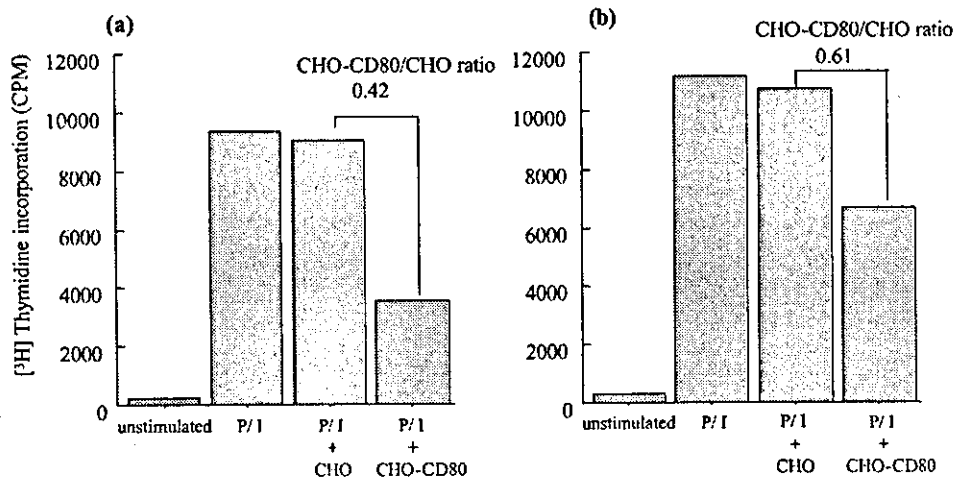


Figure 2 Representative data of T-cell proliferation assays; (a) control, (b) SLE patient (no. 15). Purified T cells were stimulated with or without PI and cultured with CHO or CHO-CD80 cells or medium alone. The CPM ratio of T-cells with CHO-CD80 to T-cells with CHO (CHO-CD80/CHO ratio) was used to determine the inhibitory effects of CTLA4.

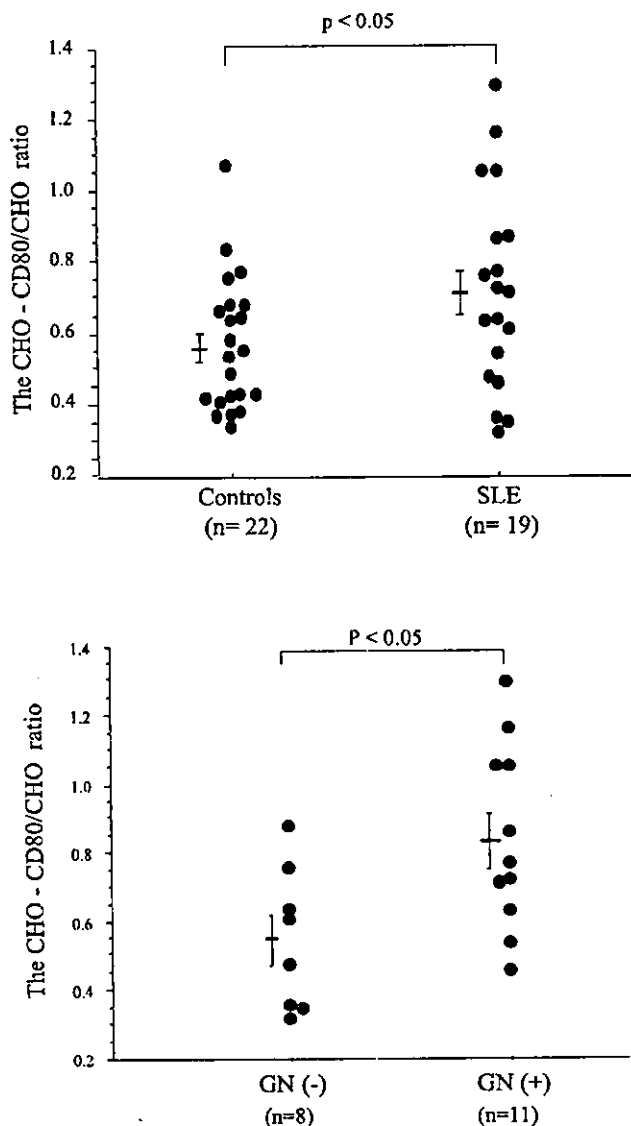


Figure 4 T-cell proliferation assay mediated by the CTLA4/CD28 ligand CD80. (a) Comparison of CHO-CD80/CHO ratio in SLE patients and controls (the CHO-CD80/CHO ratio in SLE patients ($n = 19$) is significantly higher than those of the controls ($n = 22$)). (b) Comparison of CHO-CD80/CHO ratio in SLE patients with or without glomerulonephritis (GN) (the CHO-CD80/CHO ratio in SLE patients with GN ($n = 11$) is significantly higher than those of SLE patients without GN ($n = 8$); error bars represents the mean \pm SD of the CHO-CD80/CHO ratio).

to stimulation. It is known that an abnormality in T-cell proliferation exists in SLE. To minimize these influences of T cell abnormality among SLE patients, our study comparatively investigated each CPM ratio (the CPM ratio of T cells cultured with a combination of PI with CHO-CD80 cells/the CPM ratio of T cells cultured with a combination of PI with CHO cells) instead of utilizing the CPM value directly to evaluate the proliferate function of the T cells. The decrease in

the CHO-CD80/CHO ratio revealed that CTLA4 on T-cells functioned effectively. The CHO-CD80/CHO ratio in patients with SLE was significantly higher than controls ($P < 0.05$) (Figure 4a). This data revealed that CTLA4 function, as a negative regulator on T-cell activation, was impaired in a portion of the SLE patients. Next we analysed whether an association exists between CTLA4 function and the clinical features. We revealed that the CHO-CD80/CHO ratio in SLE patients with glomerulonephritis (GN) as significantly higher than those without GN (Figure 4b). There was no significant association of additional organ involvement and these results. In addition, there was no correlation between cell surface or intracellular CTLA4 expression and the CHO-CD80/CHO ratio. One postulation is that the decrease of CTLA4 function may be related to the pathogenesis of lupus nephritis.

Discussion

The inability to generate effective down-regulatory networks of immune hyperactivity is one pathogenesis in patients with SLE. CTLA4 is one of the negative regulators of T-cell activation. However, little is known about the functional involvement of CTLA4 in human autoimmune diseases. It has been reported that CTLA4 expression on peripheral blood T-cells in SLE patients is intact at the mRNA and protein levels.²³ Although the level of surface expression of CTLA4 on CD28 positive T-cells was quite modest and no significant differences of its expression were revealed between the controls and SLE patients (Table 3), intracellular CTLA4 expression in CD28 positive T-cells was significantly greater in SLE patients than in the controls in our study. This data is consistent with other studies. In addition, surface and intracellular expression of CTLA4 was up-regulated after activation and the kinetics of cell surface CTLA4 expression paralleled the kinetics of intracellular expression (data not shown). Worthy of note is that these data suggested that CTLA4 expression is not impaired in SLE patients.

In murine relapsing experimental autoimmune encephalomyelitis (EAE), CTLA4 expression was up-regulated during acute disease activity, peaked at remission, and persisted during relapses.²⁴ In humans, there is no observation reported regarding the association between CTLA4 expression and disease activity. However, the expression of CTLA4 did not correlate to SLEDAI, serological data, nor with the specific clinical features of SLE in the majority of the patients evaluated in this study. Interpretation of this result may be complicated due to the existence of additional variables such as disease state and therapy.

CTLA4 functions as a negative regulator of T-cell activation, and was evaluated with T-cell proliferation assay inhibited by CD80 in a CTLA4-dependent manner. We demonstrated that the inhibitory effect of CTLA4 in SLE patients was inferior to those of the controls. There are several possible mechanisms including gene polymorphisms and signal transduction, to be considered as the reason why CTLA4 function was defective in spite of intact expression. The first possibility is polymorphisms of the human *CTLA4* gene. The chromosome 2q33 region, where the *CTLA4* and *CD28* genes are located,²⁵ is one of the potential susceptibility loci for human SLE.^{26,27} Recently, *CTLA4* polymorphisms in SLE patients have been reported among the Japanese and Slovak population.²⁸ *CTLA4* 49A/G and 37 (AT)_n polymorphisms among the Japanese population might have affected the *CTLA4* mRNA stability and subsequent CTLA4 expression. However, other studies together with our findings indicated that there is no apparent defective mRNA and protein expression of CTLA4 in human SLE, and these polymorphisms are unlikely to affect CTLA4 function. Other undetectable CTLA4 polymorphism involved in CTLA4 function remains to be studied.

The second possibility is that other molecules that are associated with CTLA4 may be responsible for the impairment of CTLA4 function. Recent studies have suggested that functional defects of SLE T-cells lie in the early signaling pathways between T-cell receptor (TCR) and protein kinase C.¹⁶ CTLA4 is known to be associated with the TCR complex ζ chain and CTLA4-TCR ζ interaction inhibits TCR signal transduction after T-cell activation.²⁹ It has been reported that TCR ζ chain expression in peripheral blood T-cells from SLE patients is decreased compared with the controls and systemic sclerosis patients. In addition, Src family tyrosine kinases such as Fyn and Lck regulate cell-surface expression of CTLA4 through tyrosine phosphorylation of CTLA4.²⁰ If CTLA4 is not phosphorylated, surface CTLA4 rapidly internalizes intracellularly. These reports raise the possibility that the expression and function of CTLA4 themselves are not defective, but the early signaling pathways associated with CTLA4 molecules including TCR complex ζ chain and Src family tyrosine kinases are impaired in SLE patients.

Recently, there have been studies and investigations that reported on the identification of a native soluble CTLA4 in humans. The presence of functional capability has been demonstrated and reported *in vitro* through its inhibitory actions in mixed leukocyte response, even though it has not yet been clearly defined. Soluble CTLA4 level in SLE patients has been evaluated and reported; the level of soluble CTLA4 in SLE patients was evaluated in comparison to that of

controls, but correlation to its activity was not confirmed or identified.^{30,31} In our present study, the level of CTLA4 was not evaluated in serum but was demonstrated with the T-cell proliferation assay; our study protocol utilizing the T-cell proliferation assay does not require the use of serum, therefore there was no influence of abnormal serum soluble CTLA4 in reference to our study findings. Further studies and investigations are necessary for evaluation of the level of soluble CTLA4 and its correlation to the manifestations and symptoms of the disease.

SLE is envisioned to arise from hyper-activated helper T-cells that cause polyclonal B-cell secretion of pathogenic autoantibodies and formation of immune complexes that deposit in sites such as the kidney. CTLA4 binds to CD80/CD86 with greater affinity than CD28; a soluble form of CTLA4 has been used to inhibit T-cell co-stimulation via CD28, by blocking CD80 and CD86 receptors on APCs. Blocking of this pathway has been demonstrated to inhibit autoimmunity. In rats, CTLA4Ig, which inhibited the ligation of CD28 and either CD80 or CD86 on APCs, prevented the development of experimental autoimmune glomerulonephritis.³² This data suggested that the CD80/CD86-CD28/CTLA4 co-stimulatory pathway might be involved in the pathogenesis of autoimmune nephritis. CTLA4 has been described as a physiologic inhibitor of T-cell activation, but is not involved in the pathogenesis of any human disease. In our study, CTLA4 function was impaired in SLE patients with nephritis compared with patients without lupus nephritis. From these findings, it is likely that CTLA4 is involved in the pathogenesis of lupus nephritis. Further study is required to clarify the role of CTLA4 in the pathogenesis of lupus nephritis.

References

- 1 Karandikar NJ, Vanderlugt CL, Walunas TL, Miller SD, Bluestone JA. CTLA-4: a negative regulator of autoimmune disease. *J Exp Med* 1996; 184: 783.
- 2 Tivol EA, Borriello F, Schweitzer AN, Lynch WP, Bluestone AJ, Sharpe AH. Loss of CTLA-4 leads to massive lymphoproliferation and fatal multiorgan tissue destruction, revealing a critical negative regulatory role of CTLA-4. *Immunity* 1995; 3: 541-547.
- 3 Carreno BM, Bennett F, Chau TA, Ling V, Luxenberg D, Jussif J et al. CTLA-4 (CD152) can inhibit T cell activation by two different mechanisms depending on its level of cell surface expression. *J Immunol* 2000; 165: 1352-1356.
- 4 Lenschow DJ, Walunas TL, Bluestone JA. CD28/B7 system of T cell costimulation. *Annu Rev Immunol* 1996; 14: 233-258.
- 5 Nakaseko C, Miyatake S, Iida T, Hara S, Abe R, Ohno H et al. Cytotoxic T lymphocyte antigen 4 (CTLA4) engagement delivers an inhibitory signal through the membrane-proximal region in the absence of the tyrosin motif in the cytoplasmic tail. *J Exp Med* 1999; 190: 765-774.
- 6 Waterhouse P, Penninger JM, Timms E, Wakeham A, Shahinian A, Lee KP, et al. Lymphoproliferative disorders with early lethality in mice deficient in CTLA-4. *Science* 1995; 270: 985-988.

- 7 Perrin PJ, Maldonado JH, Davis TA, June CH, Racke MK. CTLA-4 blockade enhances clinical disease and cytokine production during experimental allergic encephalomyelitis. *J Immunol* 1996; **157**: 1333.
- 8 Hurwitz AA, Sullivan TJ, Krummel MF, Sobel RA, Allison JP. Specific blockade of CTLA-4/B7 interactions results in exacerbated clinical and histological disease in an actively induced model of experimental allergic encephalomyelitis. *J Neuroimmunol* 1997; **73**: 57.
- 9 Yamagata T, Hidaka Y, Guimaraes V, Soliman M, DeGroot LJ. CTLA-4 gene polymorphism associated with Graves' disease in a Caucasian population. *J Clin Endocrinol Metab* 1995; **80**: 41.
- 10 Donner H, Rau H, Walfish PG, Braun J, Siegmund T, Finke R et al. CTLA-4 alanine-17 confers genetic susceptibility to Graves' disease and to type I diabetes mellitus. *J Clin Endocrinol Metab* 1997; **82**: 143.
- 11 Marron MP, Raffel LJ, Garchon HJ, Jacob CO, Serrano-Rios M, Martinez Larrad MT et al. Insulin-dependent diabetes mellitus (IDDM) is associated with CTLA4 polymorphisms in multiple ethnic group. *Hum Mol Genet* 1997; **6**: 1275–1282.
- 12 Ligers A, Teleshova N, Masterman T, Huang WX, Hillert J. CTLA-4 gene expression is influenced by promoter and exon 1 polymorphisms. *Genes Immun* 2001; **2**(3): 145–152.
- 13 Seidl C, Donner H, Fischer B, Usadel KH, Sefried E, Kaltwasser JP et al. CTLA4 codon 17 dimorphism in patients with rheumatoid arthritis. *Tissue Antigens* 1998; **51**: 62–66.
- 14 Kotzin BL. Systemic lupus erythematosus. *Cell* 1996; **85**: 303.
- 15 Cohen PL. T- and B-cell abnormalities in systemic lupus. *J Invest Dermatol* 1993; **100**: 69s.
- 16 Dayal AK, Kammer GM. The T cell enigma in lupus. *Arthritis Rheum* 1996; **39**: 23.
- 17 Tan EM, Cohen A, Fries JF, Masi AT, McShane DJ, Rothfield NF et al. The 1982 revised criteria for the classification of SLE. *Arthritis Rheum* 1982; **25**: 1271–1277.
- 18 Bombardier C, Glandman DD, Urowitz MB, Caron D, Chang C. Derivation of the SLEDAI. *Arthritis Rheum* 1992; **35**: 630–640.
- 19 Boulougouris G, McLeod JD, Patel YI, Ellwood CN, Walker LSK, Sansom DM. Positive and negative regulation of human T cell activation mediated by the CTLA4/CD28 ligand CD80. *J Immunol* 1998; **161**: 3919–3924.
- 20 Lindsten T, Lee KP, Harris ES, Petryniak B, Craighead N, Reynolds PJ et al. Characterization of CTLA-4 structure and expression on human T cells. *J Immunol* 1993; **151**: 3489–3499.
- 21 Lisley PS, Greene JL, Tan P, Bradshaw J, Ledbetter JA, Anasetti C et al. Coexpression of CTLA-4 and CD28 on activated T lymphocytes. *J Exp Med* 1992; **176**: 1595–1604.
- 22 Alegre ML, Noel PJ, Eisfelder BJ, Chuang E, Clark MR, Reiner SL et al. Regulation of surface and intracellular expression of CTLA-4 on mouse T cells. *J Immunol* 1996; **157**: 4762–4770.
- 23 Liu MF, Liu HS, Wang CR, Lei HY. Expression of CTLA-4 molecule in peripheral blood T lymphocytes from patients with systemic lupus erythematosus. *J Clin Immunol* 1998; **18**: 392–398.
- 24 Issazadeh S, Navikas V, Schaub M, Sayegh M, Khoury S. Kinetics of expression of costimulatory molecules and their ligands in murine relapsing experimental autoimmune encephalomyelitis in vivo. *J Immunol* 1998; **161**: 1104–1112.
- 25 Lafage-Pochitaloff M, Costello R, Couez D, Simonetti J, Mannoni P, Mawas C et al. Human CD28 and CTLA-4 Ig superfamily genes are located on chromosome 2 at bands q33–q34. *Immunogenetics* 1990; **31**: 198–201.
- 26 Moser KL, Neas BR, Salmon JE, Yu H, Gray-McGuire C, Asundi N et al. Genome scan of human systemic lupus erythematosus: evidence for linkage on chromosome 1q in African-American pedigrees. *Proc Natl Acad Sci USA* 1998; **95**: 14869–14874.
- 27 Gaffney PM, Kearns GM, Shark KB, Ortmann WA, Selby SA, Malmgren ML et al. A genome-wide search for susceptibility genes in human systemic lupus erythematosus sib-pair families. *Proc Natl Acad Sci USA* 1998; **95**: 14875–14879.
- 28 Ahmed S, Ihara K, Kanematsu S, Nakashima H, Otsuka T, Tsuzaka K et al. Association of CTLA-4 but not CD28 gene polymorphisms with systemic lupus erythematosus in the Japanese population. *Rheumatology* 2001; **40**: 662–667.
- 29 Lee KM, Chuang E, Griffin M et al. Molecular basis of T cell inactivation by CTLA-4. *Science* 1998; **282**: 2263–2266.
- 30 Oaks MK, Hallett KM, Penwell RT, Stauber EC, Warren SJ, Tector AJ. A native soluble form of CTLA4. *Cell Immunol* 2000; **201**: 144–153.
- 31 Liu MF, Wang CR, Chen PC, Fung LL. Increased expression of soluble cytotoxic T-lymphocyte-associated antigen-4 molecule in patients with systemic lupus erythematosus. *Scan J Immunol* 2003; **57**: 568–572.
- 32 Finck Bk, Linsley PS, Wofsy D. Treatment of murine lupus with CTLA4lg. *Science* 1994; **265**: 1225.

Double Filtration Plasmapheresis for the Treatment of a Rheumatoid Arthritis Patient with Extremely High Level of C-reactive Protein

Yukihiro Matsuda,^{1,2} Hiroshi Tsuda,² Yoshinari Takasaki,² and Hiroshi Hashimoto²

¹*Division of Rheumatology, Chiba Social Insurance Hospital, Chiba, and* ²*Department of Internal Medicine and Rheumatology, Juntendo University School of Medicine, Tokyo, Japan.*

Abstract: A 68-year-old-male who was diagnosed as having rheumatoid arthritis (RA) 7 years previously was admitted the Chiba Social Insurance Hospital due to general fatigue, spiking fever, and appetite loss. Blood tests showed extremely high levels of C-reactive protein (CRP, 318.5 mg/dL), and hypergammopathy (IgG 3228 mg/dL, IgA 905 mg/dL, IgM 2537 mg/dL) and high titers of rheumatoid factor (RAPA 40960X). He was diagnosed as having RA with vasculitis, according to interstitial pneumonitis, cutaneous nodules and polyneuropathy. Prednisolone (30 mg/day) was prescribed, however, myeloperoxidase-antineutrophil cytoplasmic antibody proved to be positive (86EU) and cyclophosphamide (50 mg/day) was added one week later. Additionally, IgM K-chain M-protein was revealed and the differentiation

between auto-immune and hematologic diseases was required for further drug prescriptions. Therefore, double filtration plasmapheresis (DFPP) was initiated weekly. Hematologic diseases were negated and the hypergammopathy was improved. C-reactive protein and MPO-ANCA decreased to the normal level after three sessions (IgG 1064 mg/dL, IgA 331 mg/dL, IgM 94 mg/dL, CRP 0.04 mg/dL) and the patients symptoms improved. Prednisolone was tapered and he was discharged. It was suggested that the case presented here was quite rare, having an extremely high level of CRP which was successfully managed by DFPP. **Key Words:** C-reactive protein, Double filtration plasmapheresis, Rheumatoid arthritis, myeloperoxidase-antineutrophil cytoplasmic antibody.

The cause of rheumatoid arthritis (RA) is still unknown, however, humoral factors such as immunoglobulin, rheumatoid factors, cytokine, chemokine, proteolytic enzyme, and superoxide are considered to be related with the development of the synovitis (1). Additionally, these factors interact with each other and deteriorate the disease state. Since the articular changes expand joints in a similar way to the metastasis in cancers, it is speculated that some key pathological factors are transmitted through the blood stream and or the lymphatic tissues, like metastasis. Therefore, blood purification therapies, namely, apheresis techniques, can be applied to remove such pathological factors. Double filtration plasmapheresis (DFPP) is one of the methods of apheresis applicable for the treatment of RA and it has

been reported that DFPP is effective for the management of extra-articular manifestations of RA with vasculitis (2).

We recently experienced the rare case of an RA patient with an extremely high level of C-reactive protein (CRP), who showed significant improvements after the initiation of DFPP. This article is a case report to describe the case.

CASE REPORT

The case presented is of a 68-year-old male. He was diagnosed as having RA in 1994 at the age of 61 years, and managed the condition with methotrexate (8 mg/week) and bucillamin (200 mg/day) by another institute, however, the disease activity was high with a high level of rheumatoid factor (2560–5120X RAPA). In the middle of November 2001, he presented general fatigue, spiked fever (>38°C), and appetite loss. Although the cause of these symptoms was considered to be the side-effects of the above drugs, the cessation was not effective. He was hospi-

Received February 2004; revised June 2004.

Address correspondence and reprint requests to Dr Yukihiro Matsuda, Head, Division of Rheumatology, Chiba Social Insurance Hospital, 682 Nitona-cho, Chuo-ku, Chiba city, 260-8710, Chiba Japan. Email: ymatsuda@chiba-sih.jp